Tina Bucha ![ORCID] [1], Madasu Krishna Prasad ![ORCID] [1]

Slow flow past a weakly permeable spheroidal particle in a hypothetical cell

The perspective of the current analysis is to represent the incompressible viscous flow past a low permeable spheroid contained in a fictitious spheroidal cell. Stokes approximation and Darcy's equation are adopted to govern the flow in the fluid and permeable zone, respectively. Happel's and Kuwabara's cell models are employed as the boundary conditions at the cell surface. At the fluid porous interface, we suppose the conditions of conservation of mass, balancing of pressure component at the permeable area with the normal stresses in the liquid area, and the slip condition, known as Beavers-Joseph-Saffman-Jones condition to be well suitable. A closed-form analytical expression for hydrodynamic drag on the bounded spheroidal particle is determined and therefore, mobility of the particle is also calculated, for both the case of a prolate as well as an oblate spheroid. Several graphs and tables are plotted to observe the dependence of normalized mobility on pertinent parameters including permeability, deformation, the volume fraction of the particle, slip parameter, and the aspect ratio. Significant results that influence the impact of the above parameters in the problem have been pointed out. Our work is validated by referring to previous results available in literature as reduction cases.

1. Introduction

In the increasing span of time, the evolution of fluid mechanics has raised challenges for the researchers and the scientific community. The development in the area of fluid mechanics is widely spreading due to the dependency of life on fluids.

The low permeable problem generally deals with the flow bearing very low permeability like motion in porous fluidization, the flow of a liquid mixture, motion

✉ Madasu Krishna Prasad, Email: madaspra.maths@nitrr.ac.in, kpm973@gmail.com

[1]Department of Mathematics, National Institute of Technology, Raipur-492010, Chhattisgarh, India. ORCIDs: T.B.: 0000-0002-9709-3025; M.K.P.: 0000-0002-1819-3651

in packed beds, sedimentation, fall of snow-flakes, etc. A sort of porous membrane having low permeability that allows some particular kind of particles to permeate through it is well known as a semipermeable membrane. They only let small particles like ions and molecules of water pass through them. A kind of such membrane is observed in plants and animals, through which the process of osmosis happens. As a matter of fact, evaluating their analytical solutions is very significant to know the nature of such flows.

To study the flow field, we generally adopt Stokes equations for the fluid region and Darcy's law [2] or Brinkman's equation [3] for the porous region. While handling low porosity problems Darcy's law is chosen to be appropriate, whereas Brinkman's equation helps in studying problems with higher porosity. The investigations on the flow problems in the area of porous media are being paid attention for a long time [4–9] by considering different boundary conditions at the porous interface, including no-slip and slip conditions [10, 11]. Moreover, including the Saffman's condition, the lubricating flow of a sphere nearing a porous thin slab was analyzed by Khabthani et al. [12]. Furthermore, Lai et al. [13] carried out the work discussing the simple projection technique to know the coupling of Navier-Stokes along with Darcy's flow by employing the Beavers-Joseph-Saffman condition.

In the past few years, intensive research activities have been performed to formulate the motion through a swarm of porous particles because of its application in diverging areas like filtration of the membrane, sedimentation problem, rheology of suspension, etc. On the contrary, the formulation of such problems is very difficult, as it requires the complete analysis of the tangled interaction between multiple particles to obtain the flow fields. To get rid of this difficulty, Happel [14] introduced a unit cell model technique which is one of the most effective methods for analyzing the nature of intense scattered systems and porous media. It involves the method of replacing the system of chaotic distributed particles with an array of particles confined in a fluid cell, i.e., the entire swarm is divided into various identical cells with every particle to be surrounded by a cell. Moreover, the cell volume is picked in a such a manner that the solid volume fraction in the cell is similar to the solid volume fraction of the entire assemblage. As in several practical applications, particles are never found to be in isolation, and thus, it is significant to observe the effect of neighboring particles on the motion of particles. At present, this technique is well-liked among the scientific community and researchers as it reduces the study of assemblage to analyzing a single particle and its bounded cell. Anyway, to study the effect of neighboring particles, we have to focus on the boundary conditions at the cell surface in detail. In this approach, the cell can be chosen to be of different geometry. Among them, spherical, cylindrical, and spheroidal shaped cells are conventionally used. Initially, Happel [15] and Kuwabara [16] forwarded the concept of cell method to analyze the flow through an array of particles. However, both models adopt different conditions on the cell surface. In the Happel's model, the no-slip condition

is assumed on the inner particle and the vanishing of shear stress is considered on the external cell envelope. He explained that seeing the inter-particle interactions to be bounded to the fluid surface, the cells are non-interacting and hence no work is done by the cell surface, keeping the cell boundary to be frictionless. Further, in the Kuwabara's model, the vanishing of vorticity is supposed to hold good at the cell surface. Kuwabara's model considers that no mechanical energy is to be shared between the cell and the surrounding. Although both the models are different in terms of boundary conditions, they yield almost similar results.

A considerable amount of research [17–20] on the flow past beds of porous spheroidal particles, using both Darcy and Brinkman model, have been conducted in the last few decades. Salient observations from the aforesaid studies suggest that the cell concept is a widespread technique and is currently on demand. Moreover, the use of different available boundary conditions at the cell is observed to have a prominent effect on the flow. Prakash et al. [21] formulated the flow over a cluster of porous particles where they represented the bed of particles as a cluster of uniform porous sphere wrapped by a spherical cell. In the process of solving the problem, they took into consideration both Brinkman and Darcy's law, and derived the drag expression to predict the overall permeability of the cluster of porous particles. Saad [22] implemented the cell method to analyze the steady motion of the viscous fluid through an array of the porous spherical shell along with the stress jump boundary condition. They provided the drag force expression and further, predicted that the normalized mobility of the particles relies on the permeability, the volume fraction, and the coefficient of stress jump. Prakash and Raja Shekar [23] executed the dynamic permeability of the cluster of spherical permeable particles by accounting cell model. They imposed Darcy's law for the permeable flow along with the Saffman boundary condition. Motivated by the developments in this area of research, recently numerous works addressing the problem concerning transport in porous media have been explored. Applying Happel's along with Kuwabara's boundary conditions, the MHD flow over a sphere containing fluid immersed in a spherical cell was handled by Prasad and Bucha [24]. In the latest articles by Prasad and Bucha [25, 26], an analytical study was made to examine the effect of imposed magnetic forces on the motion through a weakly permeable spherical and cylindrical particle in a cell, respectively. In their work, they adopted Darcy's law for handling the flow past a low permeable particle. Moreover, the Saffman's slip boundary condition was considered at the inner surface. They obtained the analytical expressions for the drag, the hydrodynamic permeability, and also the Kozeny constant influenced on the sphere. Using the cell technique, Khanukaeva [27] examined the micropolar flow through a spherical cell comprising an impermeable core covered with a porous shield along with a fluid envelope. She allowed different boundary conditions to be applicable at the cell surface and studied its effect on the flow. Recently, Prasad [28] worked on finding the boundary effects on an eccentric semipermeable sphere by using cell models.

In the aforementioned literature, we speculate that the shapes of the particles are considered to be of the simple spherical form. However, in numerous engineering applications, particles often possess geometry of deformed shapes which varies significantly from the sphere. The pioneering work of Stokes [29] provides a sound knowledge about the drag force experienced by a range of shapes of particles settling in stagnant media or held stationary in moving fluids. A spherical particle represents the same projected area for the flowing fluid irrespective of its orientation. But for non-spherical particles, the orientation is required for calculating their terminal settling velocity or the drag force acting on them. On the other hand, under appropriate condition, non-spherical particles have a propensity to attain a preferred or most stable orientation irrespective of their initial orientation. All these phenomena are strongly influenced not only by the shape of the particle, its size and density, fluid properties, but also by the shape and size of confining boundaries and the imposed fluid motion, etc. To acknowledge the possible effect of varying shapes, the simplest geometry is that of a spheroid. It is slightly deformed from the shape of a sphere. These spheroid particles can be described by the aspect ratio ($\varepsilon = 1 - \epsilon$), which can cover both plate-like ($\varepsilon < 1$) and cylinder-like ($\varepsilon > 1$) shapes including spheres with $\varepsilon = 1$ [30].

As a fundamental problem, obtaining the analytical solution of flow through a spheroid is of much significance and has been carried out efficaciously by several authors [31–33]. Earlier, Dassios et al. [34] implemented the cell technique to explore the Stokes flow over a spheroidal particle immersed in a vessel. There they derived the drag force executed on the particle. Ramkisson [35] included the slip condition while examining the flow over an approximate spheroidal particle. Zlatanovski [36] applied Brinkman's model to pursue the axisymmetric flow through a porous prolate spheroid and also took into consideration the eigenvalues together with the eigenfunctions for the stream function in the porous area. Deo and Datta [37] presented the slip flow on a particle of prolate spheroidal geometry. Vainshtein et al. [38] studied the creeping motion over and inside a permeable spheroid. Ramkissoon and Rahaman [39] tackled the flow of fluid over an impermeable sphere immersed in a spheroidal vessel by assuming the no-slip condition. Besides, the drag executed on the sphere covered by a spheroidal cell was evaluated. Incorporating the slip condition, Senchenko and Keh [40] scrutinized the motion of a distorted shaped sphere in an unbounded Stokes flow. Aiming to study the motion through distorted particles, Srinivasacharya [41] executed the flow through a Darcy porous shell of approximately spherical geometry by applying continuity of normal velocity, Beavers-Joseph condition, and the continuity of pressure as the boundary conditions. Chang and Keh [42] explored the translational and the rotational motion of the deformed colloidal spheres having a slip effect. Moreover, Saad [43] inscribed the translational as well as the rotational movement of the porous spheroid enclosed in a cell and also deduced the drag and the couple influenced on the particle, for the prolate as well as oblate spheroidal cases. In view of the significance of such flow, Saad [44] treated the motion of viscous fluid past

a cluster of porous spheroids confined inside a spheroidal envelope by considering different cell models. He derived the expressions for the drag and the normalized mobility on the particle and further, observed its dependence of important flow parameters by graphical simulation. Regarding the examination of the resistance force, Srinivasacharya and Prasad [45, 46] presented a study of the motion of a porous approximate sphere containing a solid core in both unbounded and bounded medium, respectively. Further, motion of a porous approximate sphere contained inside an approximate spherical container was studied by Srinivasacharya and Prasad [47]. Chen [48] made an attempt to draw out liquid from a Darcy porous medium of a slender permeable prolate spheroid. Employing the condition of Beavers-Joseph-Saffman, Rasoulzadeh and Kuchuk [49] focused on extracting the effective permeability for spherical and spheroidal vug of the porous medium comprising fracture inclusion. In an article by Yadav et al. [50], the steady flow over a porous membrane consisting of impervious spheroid wrapped with a porous layer is discussed, and thereafter, they evaluated the hydrodynamic permeability acting on the membrane. Employing the condition of Beavers-Joseph-Saffman-Jones, the viscous flow past a Darcy's governed permeable spheroid was demonstrated by Prasad and Bucha [51]. They employed the condition of balancing the normal stress in the fluid area with the pressure in the permeable area of flow. Recently, Prasad and Bucha [52] analyzed the effect of magnetic field on the flow past a porous spheroid governed by Brinkman's model and evaluated the drag force acting on the particle.

As far as we know, the work regarding the analysis of the impact of a slip on the flow past a spheroidal particle within a cell by using BJSJ condition and pressure balance with tangential stress has not been investigated earlier. The flow through particle inside a cell is the basis for the study of heat and mass transfer phenomena in swarms of spheroidal particles [34]. Moreover, such flows are considered as an idealized model for capturing the particles in the filtration comprising of connected pores. In various practical problems, the shape of the particle is not perfectly spherical. Keeping in view the importance of study in porous flows, the purpose pursued in the present work is to model the problem of flow past a deformed permeable spherical particle contained inside a cell. In the present paper, the low Reynolds flow through a permeable spheroid enveloped inside a spheroidal cell is studied, adopting Darcy's law for the motion is the permeable zone. As the fluid porous interface condition, the conditions of conservation of mass, the balancing of pressure in the permeable region to the normal stresses in the liquid region together with the Beavers-Joseph-Saffman-Jones slip condition are treated to be applicable. Moreover, Happel's and Kuwabara's cell models are employed at the cell surface. A closed solution for the drag is derived and further, the normalized mobility of the particle is also presented. Graphical and tabular results for normalized mobility on significant parameters like permeability, deformation, volume fraction, slip parameter, and aspect ratio, are obtained and discussed for both the cell models.

2. Mathematical formulation of the problem

As depicted in Fig. 1, the steady incompressible viscous flow past a permeable spheroid confined inside a fictitious spheroidal cell assuming low permeability is pursued. Stokes equation and Darcy's law are applied to analyze the motion in fluid and permeable region, respectively. Both the cases of an oblate and a prolate spheroid are illustrated. The radius of the inner spheroid is denoted as $r = a[1 + \alpha_m \, \vartheta_m(\zeta)]$ and outer cell spheroid is $r = b[1 + \alpha_m \, \vartheta_m(\zeta)]$.
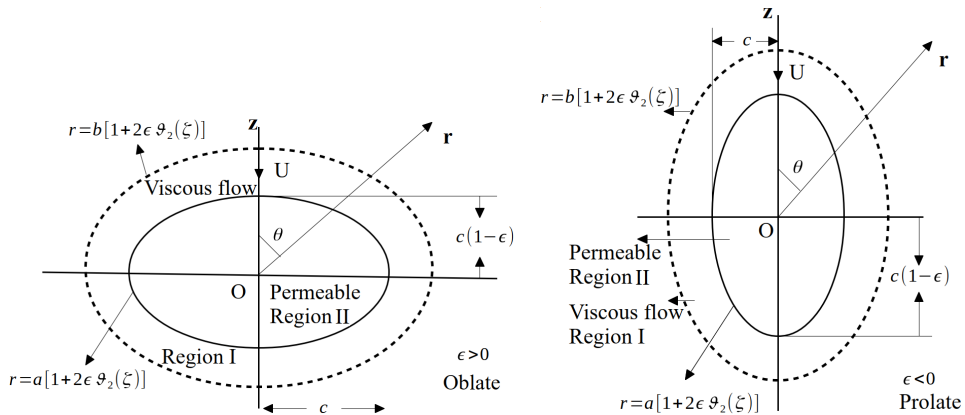

Fig. 1. Physical situation of a permeable oblate or prolate spheroid in a concentric spheroidal cell

2.1. Flow field equations

Motion of the fluid flowing in the clear fluid region as governed by Stokes approximation is

$$\nabla \cdot \vec{v}^{\,(1)} = 0, \tag{1a}$$

$$\nabla p^{(1)} + \mu \, \nabla \times \nabla \times \vec{v}^{\,(1)} = 0. \tag{1b}$$

Motion of the fluid flowing through the permeable medium is assumed to be governed by Darcy's law represented as

$$\nabla \cdot \vec{v}^{\,(2)} = 0, \tag{2a}$$

$$\nabla p^{(2)} + \frac{\mu}{k} \vec{v}^{\,(2)} = 0, \tag{2b}$$

with $\vec{v}$, p, μ, k as the velocity vector, the pressure, the viscosity coefficient and the permeability of permeable region, respectively.

For the ease of pursuing the current work, the following dimensionless variables are introduced

$$r = a \tilde{r}, \qquad \nabla = \frac{\tilde{\nabla}}{a}, \qquad \vec{v} = U \, \tilde{\vec{v}}^{\,(i)}, \qquad p = \frac{\mu \, U}{a} \tilde{p} \tag{3}$$

in the governing equation (1) and (2), and later ignoring the tildes, we have

$$\nabla \cdot \vec{v}^{(1)} = 0, \tag{4a}$$

$$\nabla p^{(1)} + \nabla \times \nabla \times \vec{v}^{(1)} = 0, \tag{4b}$$

$$\nabla \cdot \vec{v}^{(2)} = 0, \tag{5a}$$

$$\nabla p^{(2)} + \alpha^2 \vec{v}^{(2)} = 0, \tag{5b}$$

where, we denote $\alpha^2 = \dfrac{a^2}{k}$ as permeability parameter.

The spheroidal surface is supposed to be $r = a[1 + f(\theta)]$ that differs a bit from the sphere $r = a$. The orthogonality of the Gegenbauer functions $\vartheta_m(\zeta)$, $\zeta = \cos\theta$, in general circumstances, allows the expansion $f(\theta) = \displaystyle\sum_{m=2}^{\infty} \alpha_m \vartheta_m(\zeta)$, where the Gegenbauer function and Legendre function $P_n(\zeta)$ are related as

$$\vartheta_n(\zeta) = \frac{P_{n-2}(\zeta) - P_n(\zeta)}{2n-1}, \quad n \geq 2. \tag{6}$$

The spheroid surface r_a is now supposed to be $r = a[1 + \displaystyle\sum_{m=2}^{\infty} \alpha_m \vartheta_m(\zeta)]$.

Also, we suppose the coefficients α_m are small enough to have negligible effects of its squares and higher powers and hence can be ignored [14]. Therefore, $(r/a)^y \approx 1 + y\,\alpha_m\,\vartheta_m(\zeta)$, with y to be positive or negative.

2.2. Stream functions

Consider (r, θ, ϕ) to represent a co-ordinate system in spherical polar form along with unit vectors $(\vec{e}_r, \vec{e}_\theta, \vec{e}_\phi)$. According to the formulation, the flow is along the meridian plane and axisymmetric in nature, leading to all the involved quantities to be independent of ϕ. Therefore, we can now consider the velocity vector as

$$\vec{v}^{(i)} = v_r^{(i)}(r, \theta)\,\vec{e}_r + v_\theta^{(i)}(r, \theta)\,\vec{e}_\theta, \quad i = 1, 2. \tag{7}$$

Accounting the condition of incompressibility $\nabla \cdot \vec{v}^{(i)} = 0$, the stream functions $\psi^{(i)}(r, \theta)$ are represented as follows

$$v_r^{(i)} = -\frac{1}{r^2 \sin\theta} \frac{\partial \psi^{(i)}}{\partial \theta}, \qquad v_\theta^{(i)} = \frac{1}{r \sin\theta} \frac{\partial \psi^{(i)}}{\partial r}. \tag{8}$$

Eliminating the terms containing pressure in Eqs. (4) and (5), and thereafter implementing Eq. (8) in the simplified equations, we acquire

$$E^4 \psi^{(1)} = 0, \tag{9}$$

$$E^2 \psi^{(2)} = 0, \tag{10}$$

with $E^2 = \dfrac{\partial^2}{\partial r^2} + \dfrac{\sin\theta}{r^2} \dfrac{\partial}{\partial \theta} \left(\dfrac{1}{\sin\theta} \dfrac{\partial}{\partial \theta} \right)$ known as Stokes operator.

3. Boundary conditions

Different boundary conditions are offered for studying flow past permeable particles at liquid-porous interface. However, we have to specify the conditions which are found appropriate from the physical as well as mathematical view. For the low permeability problem, the interface condition at the spheroidal interface $r = a[1 + \alpha_m \vartheta_m(\zeta)]$ are the continuity of normal components of velocity, proportionality of the shear stress with the tangential velocity components, i.e., Beavers-Joseph-Saffman-Jones slip condition [7, 10, 11, 49, 51] and the normal stress acting on fluid to be identical to the pressure in the permeable area, i.e., a jump condition for pressures [49, 54].

At the spheroidal interface $r = a[1 + \alpha_m \vartheta_m(\zeta)]$, we propose the following conditions

1. Continuity of normal velocity components

$$\left(\vec{v}^{(1)} - \vec{v}^{(2)} \right) \cdot \vec{n} = 0, \tag{11}$$

2. Beavers-Joseph-Saffman-Jones condition

$$\vec{n} \cdot \tau^{(1)} \cdot \vec{s} = \frac{\mu}{\lambda \sqrt{k}} \vec{v}^{(1)} \cdot \vec{s}, \tag{12}$$

   with $\tau^{(1)}$ to be the stress tensor of viscous fluid (Region I) and λ to be the dimensionless slip parameter which relies on the nature of porous media. The value of λ lies between 0.25 and 10 [1, 11, 54]. Moreover, in the case with $\lambda = 0$ together with extremely low permeability the proposed problem reduces to the motion of fluid through a semipermeable spheroid.

3. Jump condition for pressures [49, 51, 54]

$$\vec{n} \cdot \tau^{(1)} \cdot \vec{n} = -p^{(2)}. \tag{13}$$

Also, $\vec{n} = \vec{e}_r - \alpha_m \sqrt{1 - \zeta^2} P_{m-1}(\zeta) \vec{e}_\theta$, is the unit normal vector and $\vec{s}$ is the arbitrary tangential vector at the interface of spheroid $r = a[1 + \alpha_m \vartheta_m(\zeta)]$.

Boundary conditions at infinity ($r \to \infty$) for the motion in fluid area are $v_r^{(1)} = -U \cos \theta$ and $v_\theta^{(1)} = U \sin \theta$.

Implementing the values of $\vec{n}$ and $\vec{s}$ in Eqs. (11) to (13), we get

$$v_r^{(1)} - v_r^{(2)} = \left(v_\theta^{(1)} - v_\theta^{(2)} \right) \alpha_m \sqrt{1 - \zeta^2} P_{m-1}(\zeta), \tag{14}$$

$$\tau_{r\theta}^{(1)} + \alpha_m \sqrt{1-\zeta^2} P_{m-1}(\zeta) \left(\tau_{rr}^{(1)} - \tau_{\theta\theta}^{(1)} \right) = \frac{\alpha}{\lambda} \left(v_\theta^{(1)} + v_r^{(1)} \alpha_m \sqrt{1 - \zeta^2} P_{m-1}(\zeta) \right), \tag{15}$$

$$\tau_{rr}^{(1)} - 2\alpha_m \tau_{r\theta}^{(1)} \sqrt{1 - \zeta^2} P_{m-1}(\zeta) = -p^{(2)}. \tag{16}$$

At the cell surface $r = b[1 + \alpha_m \vartheta_m(\zeta)]$, we consider the two frequently used models, referred as Happel's and Kuwabara's models. In both the models, the radial velocity on the cell surface is supposed to be continuous, i.e.,

$$v_r^{(1)} + U \cos \theta = \alpha_m \left(v_\theta^{(1)} - U \sin \theta \right) \sin \theta P_{m-1}(\zeta), \tag{17}$$

• Happel's model [15] i.e., vanishing of tangential stress

$$\tau_{r\theta}^{(1)} + \alpha_m \left(\tau_{rr}^{(1)} - \tau_{\theta\theta}^{(1)} \right) \sin \theta P_{m-1}(\zeta) = 0, \tag{18}$$

• Kuwabara's model [16] i.e., vanishing of vorticity

$$\text{curl } \vec{v}^{(1)} = 0. \tag{19}$$

All the aforementioned conditions expressed in the stream functions $\psi^{(i)}$; $i = 1, 2$. are presented below
At the surface $r = 1 + \alpha_m \vartheta_m(\zeta)$

$$\left(\frac{\partial \psi^{(1)}}{\partial \zeta} - \frac{\partial \psi^{(2)}}{\partial \zeta} \right) = r \alpha_m P_{m-1}(\zeta) \left(\frac{\partial \psi^{(1)}}{\partial r} - \frac{\partial \psi^{(2)}}{\partial r} \right), \tag{20}$$

$$2r \frac{\partial}{\partial r} \left(\frac{1}{r} \frac{\partial \psi^{(1)}}{\partial r} \right) - E^2 \psi^{(1)} + 2\alpha_m \vartheta_2(\zeta) P_{m-1}(\zeta) \left(\frac{4}{r} \frac{\partial^2 \psi^{(1)}}{\partial r \partial \zeta} - \frac{6}{r^2} \frac{\partial \psi^{(1)}}{\partial \zeta} \right.$$
$$\left. + \frac{P_1(\zeta)}{r \vartheta_2(\zeta)} \frac{\partial \psi^{(1)}}{\partial r} \right) = \frac{\alpha}{\lambda} \left(\frac{\partial \psi^{(1)}}{\partial r} + \frac{1}{r} (1 - \zeta^2) \alpha_m P_{m-1}(\zeta) \frac{\partial \psi^{(1)}}{\partial \zeta} \right), \tag{21}$$

$$- p^{(1)} - \frac{2}{r^2} \left[\frac{2}{r} \frac{\partial \psi^{(1)}}{\partial \zeta} - \frac{\partial^2 \psi^{(1)}}{\partial r \partial \zeta} \right]$$
$$- \frac{2\alpha_m P_{m-1}(\zeta)}{r} \left[2r \frac{\partial}{\partial r} \left(\frac{1}{r} \frac{\partial \psi^{(1)}}{\partial r} \right) - E^2 \psi^{(1)} \right] = -p^{(2)}, \tag{22}$$

and at the surface $r = \eta^{-1}[1 + \alpha_m \vartheta_m(\zeta)]$, with $\eta = \dfrac{a}{b}$

$$\frac{\partial \psi^{(1)}}{\partial \zeta} + r^2 \cos \theta = r \alpha_m P_{m-1}(\zeta) \left(\frac{\partial \psi^{(1)}}{\partial r} - 2r \vartheta_2(\zeta) \right), \tag{23}$$

• Happel's model:

$$2r \frac{\partial}{\partial r} \left(\frac{1}{r} \frac{\partial \psi^{(1)}}{\partial r} \right) - E^2 \psi^{(1)}$$
$$+ 2\alpha_m \vartheta_2(\zeta) \left[\frac{4}{r} \frac{\partial^2 \psi^{(1)}}{\partial r \partial \zeta} - \frac{6}{r^2} \frac{\partial \psi^{(1)}}{\partial \zeta} + \frac{P_1(\zeta)}{r \vartheta_2(\zeta)} \frac{\partial \psi^{(1)}}{\partial r} \right] P_{m-1}(\zeta) = 0, \tag{24}$$

• Kuwabara's model:

$$E^2 \psi^{(1)} = 0. \tag{25}$$

4. Solution part

Using the separation of variables method [14, 43, 44, 52], the solution for the Eqs. (9) and (10) in the viscous fluid (Region I) and permeable zone (Region II) are as follows

$$
\psi^{(1)} = \left[a_2 r^2 + \frac{b_2}{r} + c_2 r^4 + d_2 r \right] \vartheta_2(\zeta)
$$

$$
+ \sum_{n=3}^{\infty} \left[A_n r^n + B_n r^{-n+1} + C_n r^{n+2} + D_n r^{-n+3} \right] \vartheta_n(\zeta), \qquad (26)
$$

$$
\psi^{(2)} = \left(e_2 r^2 + f_2 r^{-1} \right) \vartheta_2(\zeta) + \sum_{n=3}^{\infty} \left(E_n r^n + F_n r^{-n+1} \right) \vartheta_n(\zeta). \qquad (27)
$$

The stream function $\psi^{(2)}$ is finite in the region I and imposes the condition $f_2 = 0$ and $F_n = 0$ for $n > 2$. Pressure acting in regions I and II are expressed as

$$
p^{(1)} = - \left(10 c_2 + \frac{d_2}{r^2} \right) P_1(\zeta) - \sum_{n=3}^{\infty} \left[\left(\frac{4n+2}{n-1} \right) C_n r^{n-1} + \left(\frac{4n-6}{n} \right) D_n r^{-n} P_{n-1}(\zeta) \right], \quad (28)
$$

$$
p^{(2)} = \alpha^2 \left[e_2 r P_1(\zeta) + \sum_{n=3}^{\infty} E_n \frac{r^{n-1}}{n-1} P_{n-1}(\zeta) \right]. \qquad (29)
$$

Where a_2, b_2, c_2, d_2, and e_2 are unknown constants to be determined and they contribute the solution of slow flow past a weakly permeable sphere in bounded medium. A_n, B_n, C_n, D_n, and E_n for $n > 2$ are unknown constants to be determined and they represent deformation part of the solution of slow flow past a weakly permeable spheroid in bounded medium. Initially, we evaluate the solution corresponding to the boundary $r = 1 + \alpha_m \vartheta_m(\zeta)$. The solution for the case $r = 1 + \sum_{m=2}^{\infty} \alpha_m \vartheta_m(\zeta)$. Same method is adopted for each m to obtain the stream functions for the flow regions.

5. Implementing to permeable spheroid

As a special case, flow through a prolate or an oblate permeable spheroid is studied. The equation describing the surface of the spheroid in the Cartesian frame (x, y, z) is

$$
\frac{x^2 + y^2}{c^2} + \frac{z^2}{c^2 (1 - \epsilon)^2} = 1, \qquad (30)
$$

where c to be the equatorial radius. Besides, ϵ is supposed to be so small that its squares and higher powers are ignored. In polar form, the equation describing the spheroidal surface (30) is $r = a[1 + 2\epsilon \vartheta_2(\zeta)]$, with $a = c(1 - \epsilon)$.

The spheroid behaves as an oblate spheroid for $0 < \epsilon \leq 1$, and as a prolate spheroid for $\epsilon < 0$. The condition of $\epsilon = 0$ describes the case of a sphere of radius c. To utilize the above results, we choose $m = 2$; $\alpha_m = 2\epsilon$. Thus, the stream functions are

$$\psi^{(1)} = \left[(a_2 + A_2)r^2 + (b_2 + B_2)r^{-1} + (c_2 + C_2)r^4 + (d_2 + D_2)r\right]\vartheta_2(\zeta)$$
$$+ \left[A_4 r^4 + B_4 r^{-3} + C_4 r^6 + D_4 r^{-1}\right]\vartheta_4(\zeta), \tag{31}$$

$$\psi^{(2)} = (e_2 + E_2)\, r^2 \vartheta_2(\zeta) + E_4 r^4 \vartheta_4(\zeta). \tag{32}$$

6. Hydrodynamic drag acting on the particle

On account of the viscous flow, a resisting force is exerted on the spheroidal particle inside a cell. To evaluate the drag, we adopt the following formula [14, 44, 51]

$$F_D = \int\limits_S \left(\vec{n} \cdot \tau^{(1)}\right) \cdot \vec{k}\, dS, \tag{33}$$

with $\vec{n} = \vec{e}_r - \epsilon \sin 2\theta \vec{e}_\theta$; $dS = 2\pi a^2(1 + 2\epsilon \sin^2 \theta)\sin\theta\, d\theta$ and $\vec{k}$ to be the unit vector along the z direction.

On solving the above equation providing the stress components and stream function given in Eq. (26) along with the surface $r = 1 + \epsilon \sin^2 \theta$, we obtain

$$F_D = 4\pi\mu U a(d_2 + D_2). \tag{34}$$

Utilizing the values of d_2, D_2 obtained by solving the equations obtained from boundary conditions, together with $a = c(1 - \epsilon)$ and thereafter $\alpha = \alpha_1(1 - \epsilon)$, $\eta = \eta_1(1 - \epsilon)$ [44], the ultimate equations for both the cell models are reduced as

• Happel's model

$$F_{Hp} = 4\pi\mu U c \left[\frac{\alpha_1\left(6\alpha_1\lambda\xi_1 - 2\eta_1^5\xi_2 - 3\xi_3\right)}{6\Delta_1\lambda + \Delta_2} + \frac{\epsilon\left(\Delta_3\lambda^2 + \Delta_4\lambda + \Delta_5\right)}{5\left(\Delta_6\lambda^2 + \Delta_7\lambda + \Delta_8\right)}\right], \tag{35}$$

• Kuwabara's model

$$F_{Ku} = -4\pi\mu U c \left[\frac{15\alpha_1\left(2\alpha_1\lambda + \alpha_1^2 + 4\right)}{6\delta_1\lambda + \delta_2} + \frac{\epsilon\left(\delta_3\lambda^2 + \delta_4\lambda + \delta_5\right)}{\delta_6\lambda^2 + \delta_7\lambda + \delta_8}\right]. \tag{36}$$

Where, $\alpha_1 = \dfrac{c}{\sqrt{k}}$ and $\eta_1 = \dfrac{c}{b}$. Also, the particle volume ratio of the unit cell is assumed to be identical to the particle volume fraction γ over the whole suspension. Therefore, $\gamma = \left(\dfrac{c}{b}\right)^3$, i.e., $\gamma = \eta_1^3$. Also, all the newly introduced variables are mentioned in Appendix B.

6.1. Some special results

Few significant results, evaluated in the limiting form as mentioned below, validate the consistency of the current analytical study.

Bounded by hypothetical cell

Case 1: In absence of slip, i.e., $\lambda = 0$ in Eqs. (35) and (36), it acts as flow over a semipermeable spheroid in cell model and the drag expression turns to

- Happel's model

$$F_{Hp} = 4\pi\mu U c \left[\frac{-\alpha_1 \left(3\xi_3 + 2\eta_1^5 \xi_2 \right)}{\Delta_2} + \frac{\epsilon \Delta_5}{5\Delta_8} \right], \tag{37}$$

- Kuwabara's model

$$F_{Ku} = -4\pi\mu U c \left[\frac{15\alpha_1 \left(\alpha_1^2 + 4 \right)}{\delta_2} + \frac{\epsilon \delta_5}{\delta_8} \right]. \tag{38}$$

For $\epsilon = 0$ in the above equations, the drag on the perfect semipermeable sphere is obtained.

Case 2: If the deformation parameter $\epsilon = 0$ in Eqs. (35) and (36), it reduces to flow past a permeable sphere in cell model and the drag is

- Happel's model

$$F_{Hp} = 4\pi\mu U c \left[\frac{\alpha_1 \left(6\alpha_1 \lambda \xi_1 - 2\eta_1^5 \xi_2 - 3\xi_3 \right)}{6\Delta_1 \lambda + \Delta_2} \right], \tag{39}$$

- Kuwabara's model

$$F_{Ku} = -4\pi\mu U c \left[\frac{15\alpha_1 \left(2\alpha_1 \lambda + \alpha_1^2 + 4 \right)}{6\delta_1 \lambda + \delta_2} \right]. \tag{40}$$

Case 3: If $\alpha_1 \to \infty$ in Eqs. (35) and (36), it acts as a flow past a impermeable spheroid in cell model and the drag is

- Happel's model

$$F_{Hp} = \frac{4\pi\mu U c}{(\eta_1 - 1)^2 \, (\eta_1 + 1) \, \left(2\eta_1^2 + \eta_1 + 2 \right)} \left[\frac{2\eta_1^5 + 3}{\eta_1 - 1} + \frac{2\epsilon}{5} \right.$$
$$\left. \left(\frac{3\eta_1^7 \left(4\eta_1^2 + 9\eta_1 + 14 \right) + 37\eta_1^6 + 32\eta_1^5 + 63(\eta_1^2 + \eta_1 + 1)\eta_1^2 + 3(1 + 11\eta_1)}{(\eta_1 - 1)^2 \, (\eta_1 + 1) \, \left(2\eta_1^2 + \eta_1 + 2 \right)} \right) \right], \tag{41}$$

• Kuwabara's model

$$F_{Ku} = \frac{6\pi\mu Uc}{(\eta_1-1)^3\left(\eta_1^3+3\eta_1^2+6\eta_1+5\right)}\left[5+\frac{\epsilon\left(29\eta_1^4+58\eta_1^3+87\eta_1^2+46\eta_1+5\right)}{(\eta_1-1)\left(\eta_1^3+3\eta_1^2+6\eta_1+5\right)}\right]. \quad (42)$$

The above drag expression for both the models are in good agreement with the work of Saad [44].

Case 4: If both $\epsilon = 0$ and $\alpha_1 \to \infty$, it acts as flow past a impervious sphere. The drag is

• Happel's model

$$F_{Hp} = 4\pi\mu cU\left[\frac{2\eta_1^5+3}{2\eta_1^6-3\eta_1^5+3\eta_1-2}\right], \quad (43)$$

• Kuwabara's model

$$F_{Ku} = 6\pi\mu cU\left[\frac{5}{\eta_1^6-5\eta_1^3+9\eta_1-5}\right]. \quad (44)$$

which is in supports with Happel and Brenner [14].

In absence of cell surface

Case 1: As $b \longrightarrow \infty$ or $\eta_1 = 0$ in Eqs. (35) and (36), the problem turns to flow through a permeable spheroid in an infinite expanse of flow, i.e., in unbounded medium. The drag is now of the form

$$F_\infty = -4\pi\mu Uc\left[\frac{3\alpha_1\left(2\alpha_1\lambda+\alpha_1^2+4\right)}{(6\alpha_1^2+18)\lambda+2\alpha_1^3+9\alpha_1}+\frac{\epsilon\Delta_5}{\Delta_6}\right], \quad (45)$$

Case 2: If $\lambda = 0$ in Eq. (45), the problem of flow over a semipermeable spheroid is deduced and the drag is converted as follow

$$F_\infty = 6\pi\mu Uc\left[\frac{2\left(\left(\alpha_1^2+12\right)\left(2\alpha_1^2+5\right)\epsilon-5\left(\alpha_1^2+4\right)\left(2\alpha_1^2+9\right)\right)}{5(2\alpha_1^2+9)^2}\right], \quad (46)$$

Case 3: For the deformation $\epsilon = 0$ in Eq. (45), it transform into flow past a permeable sphere and the drag is

$$F_\infty = -6\pi\mu Uc\left[\frac{4\alpha_1^2\lambda+\alpha_1(2\alpha_1^2+8)}{(6\alpha_1^2+18)\lambda+\alpha_1(2\alpha_1^2+9)}\right], \quad (47)$$

Case 4: With $\lambda = 0$ in Eq. (47), flow through a semipermeable sphere is derived and the drag is

$$F_\infty = -6\pi\mu Uc\left[\frac{2\alpha_1^2+8}{2\alpha_1^2+9}\right], \quad (48)$$

The above results are in support with the work of Prasad and Bucha [51].

Case 5: With flow through a impervious spheroid, derived by letting $\alpha_1 \to \infty$ (permeability $k = 0$), the drag expression is

$$F_\infty = -6\pi\mu U c \left[1 - \frac{\epsilon}{5}\right], \tag{49}$$

It is alike as the Stokes drag over a impervious spheroid [14].

Case 6: If $\epsilon = 0$ in Eq. (49) the flow past a solid sphere is deduced with the drag as

$$F_\infty = -6\pi\mu U c. \tag{50}$$

It is the famous expression for Stokes drag over a solid sphere [14].

6.2. Normalized mobility

The normalized mobility denoted by M, is the ratio of the drag experienced by the spheroid in the unbounded medium to the drag exerted on the spheroid in presence of cell surface [44].

Mathematically, represented as $M = \dfrac{F_\infty}{F_D}$.

- Happel's model
  Using Eqs. (35) and (45), we have

$$M_{Hp} = \frac{F_\infty}{F_{Hp}} \tag{51}$$

- Kuwabara's model
  Using Eqs. (36) and (45), we have

$$M_{Ku} = \frac{F_\infty}{F_{Ku}} \tag{52}$$

It is important to note, in the limiting case, when $\eta_1 = 0$ (i.e., $b \to \infty$) the flow past an bounded spheroid is deduced and in this case the mobility tends to $M = 1$ for any value of ϵ and α_1 with $F_D = F_\infty$. Moreover, $0 \le M < 1$ for $0 < \eta_1 \le 1$ [43, 44] where $\eta_1 = \dfrac{c}{b}$ with $c \le b$. For $\alpha_1 \to \infty$, we obtain the results for impermeable solid spheroid bounded by a cell. Therefore, the expression for drag in unbounded medium reduces as given in Eq. (49) and for cell case as represented in Eqs. (41) and (42).

In this case, the particle mobility for both the models are obtained as

- Happel's model

$$M_{Hp} = \frac{1}{(1 + (2/3)\gamma^{5/3})} \left[\left(1 + (3/2)\gamma^{5/3} - (3/2)\gamma^{1/3} - \gamma^2\right)\right.$$
$$\left. + \epsilon\gamma^{1/3}\left(\frac{\left(\gamma^{1/3} - 1\right)^2\left(\gamma + 2\gamma^{2/3} + 3\gamma^{1/3} + (3/2)\right)\left(14\gamma^{5/3} + 15\gamma^{2/3} + 21\right)}{15(1 + (2/3)\gamma^{5/3})}\right)\right], \tag{53}$$

• Kuwabara's model

$$M_{Ku} = \left(1-(9/5)\gamma^{1/3}+\gamma-(1/5)\gamma^2\right)+\epsilon\left((9/5)\gamma^{1/3}-3\gamma+(6/5)\gamma^2\right). \quad (54)$$

The above expressions are in support with the results by Saad [44]. Moreover, for the case of perfect sphere i.e., $\epsilon = 0$ the results for both the models coincides with the results given by Vasin et al. [19].

7. Numerical representation and discussion

In this part, the dependence of normalized mobility M (M_{Hp} is normalized mobility for Happel's cell model, M_{Ku} is normalized mobility for Kuwabara's cell model) of the spheroidal particle on various influential parameters are illustrated through the graphs in Figs. 2 to 7. The dimensionless parameters involved in the analysis are permeability parameter k_1, slip parameter λ, particle volume fraction γ, deformation parameter ϵ.

(a) $\epsilon = -0.1$　　　　　　　　(b) $\epsilon = 0.1$
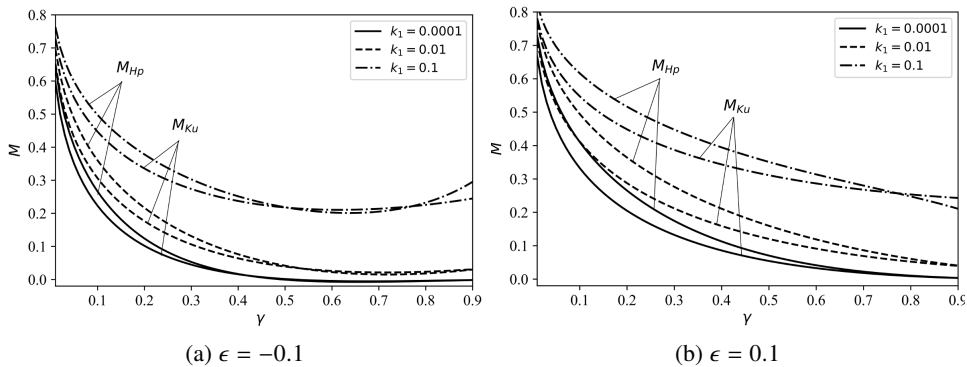
Fig. 2. Plot of normalized mobility versus particle volume fraction with $\lambda = 3$ for varying permeability

In Fig. 2, the behavior of normalized mobility according to the change in permeability and particle volume fraction for both Happel's and Kuwabara's model are shown. It delineates M_{Hp} and M_{Ku} to be a decreasing function of γ. The curves in the graph Fig. 2a is the case for flow past a prolate spheroid ($\epsilon = -0.1$) whereas Fig. 2b is for the flow past an oblate spheroid ($\epsilon = 0.1$). All the plots reveal normalized mobility to be monotonically increasing with advancing permeability. It is found that the effect of the particle interaction on mobility is more for the smaller permeability. For, $k_1 = 0.001$, the normalized mobility is nearly close to the case of a solid spheroid with a smaller value of γ, i.e., the particles are far from each other. But as the particle nears one another, their difference increases significantly and further when they are very close, there develops a huge pressure

gradient which in turn allows more fluid to flow through the permeable medium [17, 44]. The curves suggest normalized mobility to be more for the Happel's model in comparison with the Kuwabara's model. Fig. 3 depicts the impact of slip (λ) on the mobility of the particle against particle volume fraction. The graphs indicate that both the models result in almost similar qualitative behavior but a slight differing in magnitude. It may be noted that in the complete range of γ, the value of M_{Hp} and M_{Ku} enhances with the increasing value of slip. The curve for $\lambda = 0$ is the case having no slip and it represents the flow past a semipermeable spheroid. Fig. 4 demonstrates the influence of deformation on the mobility with varying particle volume fraction with the remaining parameters to have fixed values. Mobility is observed to be advancing with an increasing ϵ. Using the cell model method, it is perceived that the mobility of the permeable sphere ($\epsilon = 0$) inside a container of the identical equatorial radius is less than the mobility of an oblate spheroid and higher than the prolate spheroid. It is so because, for $\epsilon < 0$, i.e., aspect ratio exceeds 1, the major portion of the fluid slip at the particle surface occurs in the direction of the particle's movement. For $\epsilon > 0$, i.e., aspect ratio is smaller than one, the main component of the fluid slip at the surface of a spheroidal

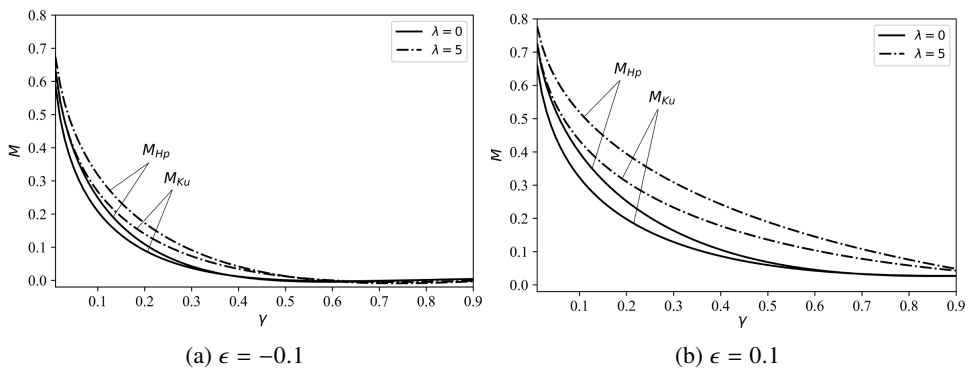(a) $\epsilon = -0.1$ (b) $\epsilon = 0.1$

Fig. 3. Plot of normalized mobility versus particle volume fraction with $k_1 = 0.001$ for varying slip
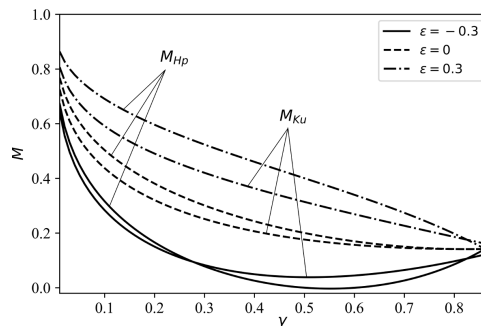

Fig. 4. Plot of normalized mobility versus particle volume fraction
with $\lambda = 3$ and $k_1 = 0.05$ for varying deformation

particle is in the direction normal to the motion of the spheroid [55]. Thus, the flow past a particle highly depends on the nature of fluid and shape of the particle, deformation of the particle, i.e., aspect ratio, and the drag is different for different shapes and fluids. A similar behavior of flow past a porous spheroid governed by Brinkman media is observed by Saad [43]. Additionally, for a fixed ϵ, the mobility of the particle even doesn't vanish for the case in which the neighboring particles touch each other (as $\gamma \to 1$). All the graphs in Fig. 5 and 6 emphasize the plots of mobility against permeability for varying γ and λ, respectively for both Happel's and Kuwabara's models. As predicted, the graphs show the mobility to be a decreasing function of γ and an increasing function of λ. In general, the mobility is found to be comparatively larger for oblate spheroids ($\epsilon = 0.1$) than the prolate ones ($\epsilon = -0.1$). From Fig. 7, one can speculate the characteristic of the mobility of the particle depending on the aspect ratio $(1 - \epsilon)$ for varying permeability. It is evident from the plot that for the spheroid with a fixed aspect ratio, mobility increases monotonically with increasing permeability for both the models [44].
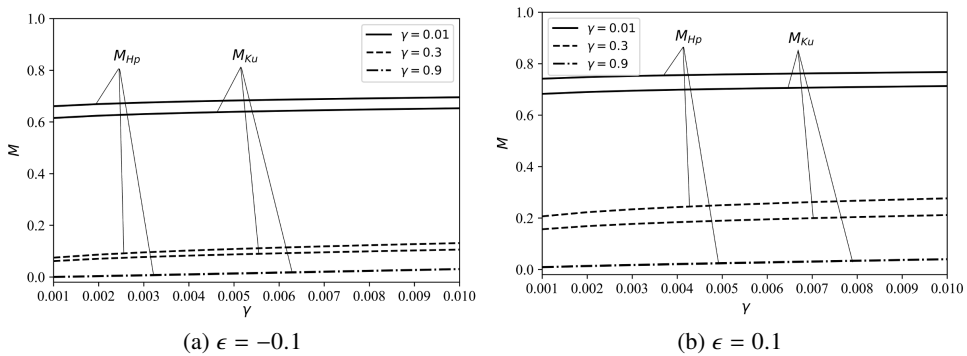

(a) $\epsilon = -0.1$ (b) $\epsilon = 0.1$

Fig. 5. Plot of normalized mobility versus permeability with $\lambda = 3$ for varying particle volume fraction

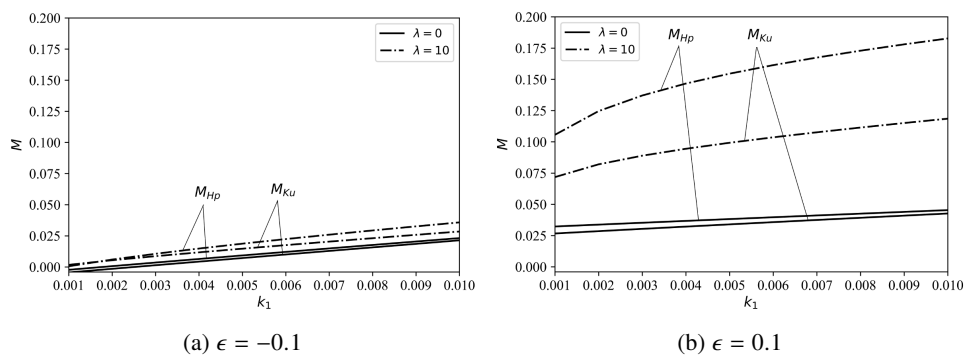(a) $\epsilon = -0.1$ (b) $\epsilon = 0.1$

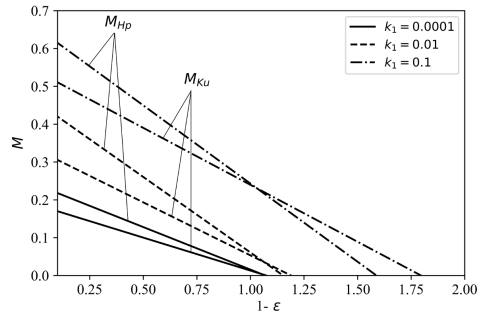Fig. 6. Plot of normalized mobility versus permeability with $\gamma = 0.6$ for varying slip

Fig. 7. Plot of normalized mobility versus aspect ratio with $\gamma = 0.6$ and $\lambda = 2$ for varying permeability

Numerical results are displayed in Tables 1 to 3, showing the dependency of normalized mobility on the dimensionless parameters for both the cell models. In Table 1, the quantitative values of mobility for altering deformation along with permeability is shown. The table shows the inferred mobility to be an increasing function of the permeability. Further, it is figured out that the mobility increases with increasing deformity, and also, the values corresponding to $\epsilon = 0$ are the results for the case of spherical particles. Moreover, mobility is observed to be higher for an oblate spheroidal particle. Table 2 illustrates the influence of altering particle volume fraction on the mobility versus permeability. We noted that the mobility decreases by increasing γ. Table 3 depicts the variation in mobility for enhancing slip in relation to permeability. It is perceived that the mobility of the particle with no-slip ($\lambda = 0$) condition is lower as compared to the mobility of the

Table 1.

Normalized mobility against permeability for flow past permeable spheroid for varying deformation with $\gamma = 0.15$ and $\lambda = 5$

k_1	$\epsilon = -0.3$	$\epsilon = -0.1$	$\epsilon = 0$	$\epsilon = 0.1$	$\epsilon = 0.3$
M_{Hp}					
0.001	0.08736	0.23395	0.30724	0.38053	0.52712
0.005	0.14089	0.28335	0.35457	0.42580	0.56826
0.01	0.17084	0.31015	0.37981	0.44947	0.58878
0.05	0.26936	0.39955	0.46464	0.52974	0.65993
0.1	0.33863	0.46307	0.52526	0.58748	0.71190
M_{Ku}					
0.001	0.08187	0.19220	0.24736	0.30253	0.41285
0.005	0.12273	0.23216	0.28688	0.34159	0.45103
0.01	0.14610	0.25474	0.30906	0.36338	0.47202
0.05	0.23254	0.34025	0.39410	0.44796	0.55567
0.1	0.30123	0.40787	0.46119	0.51451	0.62115

Table 2.

Normalized mobility against permeability for flow past permeable spheroid for varying particle volume fraction with $\epsilon = 0.1$ and $\lambda = 5$

k_1	$\gamma = 0.01$	$\gamma = 0.1$	$\gamma = 0.3$	$\gamma = 0.6$	$\gamma = 0.8$
M_{Hp}					
0.001	0.75055	0.45826	0.22963	0.07716	0.02801
0.005	0.76908	0.49859	0.28052	0.11821	0.05460
0.01	0.77858	0.51944	0.30849	0.14513	0.07587
0.05	0.81065	0.58963	0.40761	0.25834	0.18400
0.1	0.83384	0.64001	0.48019	0.34760	0.27633
M_{Ku}					
0.001	0.69308	0.37610	0.17266	0.05678	0.02158
0.005	0.71480	0.41371	0.21015	0.08381	0.04096
0.01	0.72607	0.43419	0.23270	0.10373	0.05848
0.05	0.76502	0.51085	0.32976	0.20899	0.16503
0.1	0.79362	0.56997	0.41012	0.30339	0.26472

Table 3.

Normalized mobility against permeability for flow past permeable spheroid for varying slip with $\epsilon = 0.1$ and $\gamma = 0.15$

k_1	$\lambda = 0$	$\lambda = 1$	$\lambda = 2$	$\lambda = 7$	$\lambda = 10$
M_{Hp}					
0.001	0.31020	0.32932	0.34529	0.39718	0.41597
0.005	0.31209	0.35118	0.37835	0.44378	0.46149
0.01	0.31436	0.36680	0.39925	0.46664	0.48269
0.05	0.32931	0.43278	0.47757	0.54417	0.55644
0.1	0.34245	0.48340	0.53425	0.60120	0.61256
M_{Ku}					
0.001	0.24318	0.25952	0.27305	0.31625	0.33157
0.005	0.24605	0.27952	0.30242	0.35615	0.37033
0.01	0.24948	0.29461	0.32198	0.37725	0.39008
0.05	0.27190	0.36455	0.40356	0.46002	0.47020
0.1	0.29134	0.42181	0.46760	0.52641	0.53620

particle with some slip effect. In all the tables, it is clearly described that the value of normalized mobility is higher for the Happel's cell model. It is due to the vanishing of vorticity in the Kuwabara's model, which produces a larger energy dissipation in the cell as compared to the Happel's model, which is due to the vanishing of shear stress. Further, in Kuwabara's model, an exchange of mechanical energy between the cell and the environment takes place but in Happel's model no such exchange

of mechanical energy is seen. However, the difference between both the models is very narrow.

From the above discussions, one can speculate that the dimensionless units possess a substantial impact on the flow of the permeable spheroidal particle. Further, the effect of slip is found to be dominant while pursuing problems using low permeability.

8. Conclusions

In this article, a detailed inspection of flow past a deformed permeable spherical particle surrounded by a cell is performed analytically using Stokes and Darcy's law. We have derived an analytical drag expression on the considered deformed particle possessing low permeability for both Happel's and Kuwabara's models. Several results corresponding to reduction cases matching with earlier work are included for validating the present work. The behavior of normalized mobility according to varying deformation, permeability, particle volume fraction, slip, and the aspect ratio, are illustrated through graphs and tables.

The following conclusions are made from the ongoing analysis:

- The normalized mobility of the permeable spheroidal particle in a spheroidal vessel is found to be larger for an oblate spheroid than the prolate spheroid and a sphere inside a spherical vessel of the equal equatorial radius. But, the mobility for the prolate spheroidal particle is lower than the sphere inside a vessel.
- The numerical value of mobility for the Happel's model is observed to be higher than that for the Kuwabara's model. However, they possess almost similar qualitative behavior.
- Mobility is perceived to be an increasing function of permeability, deformation, slip and it decreases with increasing values of particle volume fraction.
- The current work is capable of capturing the slip effect on the flow characteristics of a low permeable spheroidal particle.

A. Appendix

On applying the Eqs. (20) to (25) up to the first order of α_m and neglecting the other terms, we derived the equations below [52, 55]

$$(a_2 + b_2 + c_2 + d_2 - e_2) P_1(\zeta) + \alpha_m(2a_2 - b_2 + 4c_2 + d_2 - 2e_2)[\vartheta_m(\zeta)P_1(\zeta)$$

$$+ \vartheta_2(\zeta)P_{m-1}(\zeta)] + \sum_{n=3}^{\infty}(A_n + B_n + C_n + D_n - E_n)P_{n-1}(\zeta) = 0, \qquad (55)$$

$$[-2\alpha\, a_2 + (6\lambda + \alpha)b_2 + 2(3\lambda - 2\alpha)c_2 - \alpha\, d_2]\,\vartheta_2(\zeta)$$

$$- \alpha_m\, [(2\alpha\, a_2 + 2(9\lambda + \alpha)b_2 - 12(\lambda - \alpha)c_2)\,\vartheta_m(\zeta)\vartheta_2(\zeta)$$

$$- (2\alpha\, a_2 + 2\,(9\lambda + \alpha)\,b_2 - 2(6\lambda - \alpha)c_2 + 2(3\lambda + \alpha)d_2)\,\vartheta_2(\zeta)P_1(\zeta)P_{m-1}(\zeta)]$$

$$+ \sum_{n=3}^{\infty} \Big[(2n(n-2)\lambda - \alpha\, n)\, A_n - \big(2(1-n^2)\lambda + \alpha(1-n)\big)\, B_n$$

$$- \big(2(1-n^2)\lambda + \alpha(n+2)\big)\, C_n - (2n(2-n)\lambda + \alpha(3-n))\, D_n\Big]\,\vartheta_n(\zeta) = 0, \quad (56)$$

$$(6b_2 + 6c_2 + 3d_2 + \alpha^2 e_2)P_1(\zeta) + \alpha_m[-12b_2 + 18c_2 - 6d_2 + \alpha^2 e_2]\vartheta_m(\zeta)P_1(\zeta)$$

$$- 12\alpha_m(b_2 + c_2)[\vartheta_2(\zeta)P_{m-1}(\zeta) + \vartheta_m(\zeta)P_1(\zeta)] + \sum_{n=3}^{\infty} [2(2-n)A_n + 2(n+1)B_n$$

$$+ \left(\frac{2(3n - n^2 + 1)}{n}\right)C_n + \left(\frac{2(n^2 + n - 3)}{n}\right)D_n + \left(\frac{\alpha^2}{n-1}\right)E_n\Big]\, P_{n-1}(\zeta) = 0, \quad (57)$$

$$\left(\eta^{-2}a_2 + \eta b_2 + \eta^{-4}c_2 + \eta^{-1}d_2 - \eta^{-2}\right)P_1(\zeta) + \alpha_m(2\eta^{-2}a_2 - \eta b_2 + 4\eta^{-4}c_2$$

$$+ \eta^{-1}d_2 - 2\eta^{-2})[\vartheta_m(\zeta)P_1(\zeta) + \vartheta_2(\zeta)P_{m-1}(\zeta)]$$

$$+ \sum_{n=3}^{\infty} [\eta^{-n}A_n + \eta^{n-1}B_n + \eta^{-n-2}C_n + \eta^{n-3}D_n]P_{n-1}(\zeta) = 0, \quad (58)$$

$$\left(6\eta^3 b_2 + 6\eta^{-2}c_2\right)\vartheta_2(\zeta) + \alpha_m \Big[(-18\eta^3 b_2 + 12\eta^{-2}c_2)\vartheta_m(\zeta)\vartheta_2(\zeta) + 2(9\eta^3 b_2$$

$$- 6\eta^{-2}c_2 + 3\eta d_2)\vartheta_2(\zeta)P_1(\zeta)P_{m-1}(\zeta)\Big] + \sum_{n=3}^{\infty} [2n(n-2)\eta^{-n+2}A_n$$

$$+ 2(n^2 - 1)\eta^{n+1}B_n + 2(n^2 - 1)\eta^{-n}C_n + 2n(n-2)\eta^{n-1}D_n]\vartheta_n(\zeta) = 0, \quad (59)$$

$$\left(10\eta^{-2}c_2 - 2\eta d_2\right)\vartheta_2(\zeta) + \alpha_m \Big[20\eta^{-2}c_2 + 2\eta d_2\Big]\,\vartheta_m(\zeta)\vartheta_2(\zeta)$$

$$+ \sum_{n=3}^{\infty} [(4n+2)\eta^{-n}C_n - (4n-6)\eta^{n-1}D_n]\vartheta_n(\zeta) = 0. \quad (60)$$

The leading terms of the above equations are equated to zero and we have

$$a_2 + b_2 + c_2 + d_2 - e_2 = 0, \quad (61)$$

$$- 2\alpha\, a_2 + (6\lambda + \alpha)b_2 + 2(3\lambda - 2\alpha)c_2 - \alpha\, d_2 = 0, \tag{62}$$

$$6b_2 + 6c_2 + 3d_2 + \alpha^2 e_2 = 0, \tag{63}$$

$$\eta^{-2}a_2 + \eta b_2 + \eta^{-4}c_2 + \eta^{-1}d_2 - \eta^{-2} = 0, \tag{64}$$

$$6\eta^3 b_2 + 6\eta^{-2}c_2 = 0, \tag{65}$$

$$10\eta^{-2}c_2 - 2\eta d_2 = 0. \tag{66}$$

Solving these system of equations, the values of a_2, b_2, c_2, d_2, and e_2 are obtained.
Now, Eqs. (55) to (60) are

$$\sum_{n=3}^{\infty} (A_n + B_n + C_n + D_n - E_n)P_{n-1}(\zeta)$$
$$+ \alpha_m \Omega_1 \left[\vartheta_m(\zeta)P_1(\zeta) + \vartheta_2(\zeta)P_{m-1}(\zeta) \right] = 0, \tag{67}$$

$$\sum_{n=3}^{\infty} \Big[(2n(n-2)\lambda - \alpha\, n)\, A_n - \big(2(1-n^2)\lambda + \alpha(1-n)\big)\, B_n$$
$$- \big(2(1-n^2)\lambda + \alpha(n+2)\big)\, C_n - (2n(2-n)\lambda + \alpha(3-n))\, D_n \Big] \vartheta_n(\zeta)$$
$$+ \alpha_m \left[\Omega_2 \vartheta_m(\zeta)\vartheta_2(\zeta) + \Omega_3 \vartheta_2(\zeta)P_1(\zeta)P_{m-1}(\zeta) \right] = 0, \tag{68}$$

$$\sum_{n=3}^{\infty} \left[2(2-n)A_n + 2(n+1)B_n + \left(\frac{2(3n - n^2 + 1)}{n} \right) C_n \right.$$
$$\left. + \left(\frac{2(n^2 + n - 3)}{n} \right) D_n + \left(\frac{\alpha^2}{n-1} \right) E_n \right] P_{n-1}(\zeta)$$
$$+ \alpha_m \Omega_5 \vartheta_m(\zeta)P_1(\zeta) - \alpha_m \Omega_4 [\vartheta_2(\zeta)P_{m-1}(\zeta) + \vartheta_m(\zeta)P_1(\zeta)] = 0, \tag{69}$$

$$\sum_{n=3}^{\infty} [\eta^{-n}A_n + \eta^{n-1}B_n + \eta^{-n-2}C_n + \eta^{n-3}D_n]P_{n-1}(\zeta)$$
$$+ \alpha_m \Omega_6 [\vartheta_m(\zeta)P_1(\zeta) + \vartheta_2(\zeta)P_{m-1}(\zeta)] = 0, \tag{70}$$

$$\sum_{n=3}^{\infty} \Big[2n(n-2)\eta^{-n+2}A_n + 2(n^2-1)\eta^{n+1}B_n + 2(n^2-1)\eta^{-n}C_n + 2n(n-2)\eta^{n-1}D_n \Big] \vartheta_n(\zeta)$$
$$+ \alpha_m \left[\Omega_7 \vartheta_m(\zeta)\vartheta_2(\zeta) + 2\Omega_8 \vartheta_2(\zeta)P_1(\zeta)P_{m-1}(\zeta) \right] = 0, \tag{71}$$

$$\sum_{n=3}^{\infty} \Big[(4n+2)\eta^{-n}C_n - (4n-6)\eta^{n-1}D_n \Big] \vartheta_n(\zeta) + \alpha_m \Omega_9 \vartheta_m(\zeta)\vartheta_2(\zeta) = 0. \tag{72}$$

where

$$\Omega_1 = 2a_2 - b_2 + 4c_2 + d_2 - 2e_2, \quad \Omega_2 = -(2\alpha\, a_2 + 2(9\lambda + \alpha)b_2 - 12(\lambda - \alpha)c_2),$$

$$\Omega_3 = 2\alpha\, a_2 + 2(9\lambda + \alpha)b_2 - 2(6\lambda - \alpha)c_2 + 2(3\lambda + \alpha)d_2, \quad \Omega_4 = 12a_2 + 12c_2,$$

$$\Omega_5 = -12b_2 + 18c_2 - 6d_2 + \alpha^2 e_2, \quad \Omega_6 = 2\eta^{-2}a_2 - \eta b_2 + 4\eta^{-4}c_2 + \eta^{-1}d_2 - 2\eta^{-2},$$

$$\Omega_7 = -18\eta^3 b_2 + 12\eta^{-2}c_2, \quad \Omega_8 = 9\eta^3 b_2 - 6\eta^{-2}c_2 + 3\eta d_2, \quad \Omega_9 = 20\eta^{-2}c_2 + 2\eta d_2.$$

In order to calculate the arbitrary constants A_n, B_n, C_n, D_n and E_n, we require the following identities

$$\vartheta_m(\zeta)\vartheta_2(\zeta) = -\frac{(m-2)(m-3)}{2(2m-1)(2m-3)}\vartheta_{m-2}(\zeta) + \frac{m(m-1)}{(2m+1)(2m-3)}\vartheta_m(\zeta)$$
$$-\frac{(m+1)(m+2)}{2(2m-1)(2m+1)}\vartheta_{m+2}(\zeta), \tag{73}$$

$$\vartheta_m(\zeta)P_1(\zeta) + P_{m-1}(\zeta)\vartheta_2(\zeta) = -\frac{(m-2)(m-3)}{2(2m-1)(2m-3)}P_{m-3}(\zeta)$$
$$+\frac{m(m-1)}{(2m+1)(2m-3)}P_{m-1}(\zeta) - \frac{(m+1)(m+2)}{2(2m-1)(2m+1)}P_{m+1}(\zeta), \tag{74}$$

$$P_1(\zeta)\vartheta_2(\zeta)P_{m-1}(\zeta) = -\frac{(m-1)(m-2)(m-3)}{2(2m-1)(2m-3)}\vartheta_{m-2}(\zeta)$$
$$+\frac{m(m-1)}{2(2m+1)(2m-3)}\vartheta_m(\zeta) + \frac{m(m+1)(m+2)}{2(2m-1)(2m+1)}\vartheta_{m+2}(\zeta), \tag{75}$$

$$\vartheta_m(\zeta)P_1(\zeta) = \frac{(m-2)}{(2m-1)(2m-3)}P_{m-3}(\zeta) + \frac{1}{(2m+1)(2m-3)}P_{m-1}(\zeta)$$
$$-\frac{(m+1)}{(2m-1)(2m+1)}P_{m+1}(\zeta). \tag{76}$$

Solving Eqs. (67) to (72) using the above identities, we see that the values of A_n, B_n, C_n, D_n and $E_n = 0$ for $n \neq m-2, m, m+2$.

For $n = m-2, m, m+2$, the following expressions are derived

$$A_n + B_n + C_n + D_n - E_n + \Omega_1\,\overline{a}_n = 0, \tag{77}$$

$$(2n(n-2)\lambda - \alpha\, n)\,A_n - \left(2(1-n^2)\lambda + \alpha(1-n)\right)B_n$$
$$-\left(2(1-n^2)\lambda + \alpha(n+2)\right)C_n - (2n(2-n)\lambda + \alpha(3-n))\,D_n$$
$$+\Omega_2\,\overline{a}_n + \Omega_3\,\overline{b}_n = 0, \tag{78}$$

$$2(2-n)A_n + 2(n+1)B_n + \left(\frac{2(3n - n^2 + 1)}{n}\right)C_n + \left(\frac{2(n^2 + n - 3)}{n}\right)D_n$$

$$+ \left(\frac{\alpha^2}{n-1}\right)E_n - \Omega_4\,\bar{a}_n + \Omega_5\,\bar{c}_n = 0, \quad (79)$$

$$\eta^{-n}A_n + \eta^{n-1}B_n + \eta^{-n-2}C_n + \eta^{n-3}D_n + \Omega_6\,\bar{a}_n = 0, \quad (80)$$

$$2n(n-2)\eta^{-n+2}A_n + 2(n^2 - 1)\eta^{n+1}B_n + 2(n^2 - 1)\eta^{-n}C_n$$

$$+ 2n(n-2)\eta^{n-1}D_n + \Omega_7\,\bar{a}_n + 2\Omega_8\,\bar{b}_n = 0, \quad (81)$$

$$(4n+2)\eta^{-n}C_n - (4n-6)\eta^{n-1}D_n + \Omega_9\,\bar{a}_n = 0. \quad (82)$$

where

$$\bar{a}_n = \frac{n(n-1)\alpha_n}{(2n+1)(2n-3)}, \quad \bar{b}_n = \frac{n(n-1)\alpha_n}{2(2n+1)(2n-3)}, \quad \bar{c}_n = \frac{\alpha_n}{(2n+1)(2n-3)}.$$

Solving Eqs. (77) to (82), the individual values of A_n, B_n, C_n, D_n, and E_n are determined for $n = m - 2, m, m + 2$.

B. Appendix

The expression for the variables mentioned are below:

$$\xi_1 = \eta_1{}^5 - 1, \quad \xi_2 = \alpha_1{}^2 - 6, \quad \xi_3 = \alpha_1{}^2 + 4, \quad \xi_4 = \alpha_1{}^2 + 2, \quad \xi_5 = \alpha_1{}^2 + 3,$$

$$\xi_6 = 2\alpha_1{}^2 + 9, \quad \xi_7 = \alpha_1{}^2 - 15, \quad \xi_8 = \eta_1{}^5 - 2, \quad \xi_9 = 6\eta_1 - 1, \quad \xi_{10} = \alpha_1{}^2 + 6,$$

$$\xi_{11} = \alpha_1{}^2 + 24, \quad \xi_{12} = \alpha_1{}^2 + 12, \quad \xi_{13} = 2\alpha_1{}^2 + 5, \quad \xi_{14} = \alpha_1{}^4 + 39\alpha_1{}^2 - 54,$$

$$\xi_{15} = \alpha_1{}^4 - 21\alpha_1{}^2 + 216, \quad \xi_{16} = \alpha_1{}^4 + 19\alpha_1{}^2 + 36, \quad \xi_{17} = 3\xi_3 - 2\eta_1{}^{10}\xi_2,$$

$$\xi_{18} = \eta_1{}^4\xi_{14} + 3\alpha_1{}^2\xi_{11}, \quad \xi_{19} = 3\left(3\xi_3 - 2\eta_1{}^{10}\xi_2\right) + 5\eta_1{}^2\xi_1\xi_{10},$$

$$\xi_{20} = 39\eta_1{}^5 - 20\eta_1{}^2 - 24, \quad \xi_{21} = 24\xi_3 - 4\left(\alpha_1{}^2 + 39\right)\eta_1{}^5 - 5\left(5\alpha_1{}^2 + 22\right)\eta_1{}^2,$$

$$\xi_{22} = 7\alpha_1{}^4 + 64\alpha_1{}^2 + 168, \quad \xi_{23} = \alpha_1{}^4 + 12\alpha_1{}^2 - 300,$$

$$\xi_{24} = 31\alpha_1{}^4 + 342\alpha_1{}^2 + 1440, \quad \xi_{25} = 29\alpha_1{}^2\left(\alpha_1{}^2 - 2\right) - 936,$$

$$\xi_{26} = 9\xi_3 + 12\eta_1{}^5\xi_2 - 10\eta_1{}^2\xi_{10}, \quad \xi_{27} = \xi_{24} - 3\eta_1{}^5\xi_{23},$$

$$\xi_{28} = 3\eta_1{}^3\xi_2 - 5\xi_{10}, \quad \Delta_1 = \xi_1\left(\alpha_1{}^2\eta_1 - \xi_5\right),$$

$$\Delta_2 = \alpha_1\left(\xi_6 + \eta_1\left(3\eta_1{}^4\xi_4 - 3\xi_3 - 2\eta_1{}^5\xi_2\right)\right),$$

$$\Delta_3 = -36\alpha_1{}^2 \left(-\alpha_1{}^2 \xi_9 + \eta_1{}^5 \left(\xi_7 - 6\alpha_1{}^2 \eta_1\right) \xi_8 - 15\right),$$

$$\Delta_4 = 12\alpha_1 \left(2\alpha_1{}^2 \eta_1 \xi_{19} - 2\eta_1{}^6 \xi_{18} + 3\xi_{16} - \eta_1{}^5 \xi_{15}\right),$$

$$\Delta_5 = \alpha_1{}^2 \left(6\eta_1 \xi_{26} \xi_3 + 8\eta_1{}^8 \xi_2 \xi_{28} - 2\eta_1{}^5 \xi_{27} + 3\xi_{12} \xi_{13}\right), \quad \Delta_6 = 36\Delta_1{}^2,$$

$$\Delta_7 = -12\alpha_1 \Delta_1 \left(-\xi_6 - 3\eta_1{}^5 \xi_4 + 3\eta_1 \xi_3 + 2\eta_1{}^6 \xi_2\right),$$

$$\Delta_8 = \alpha_1{}^2 \left(-\xi_6 - 3\eta_1{}^5 \xi_4 + 3\eta_1 \xi_3 + 2\eta_1{}^6 \xi_2\right)^2, \quad \delta_1 = \alpha_1{}^2 \left(\eta_1{}^6 - 6\eta_1 + 5\right) + 15,$$

$$\delta_2 = \alpha_1 \left(5\xi_6 - 2\eta_1 \left(9\xi_3 + \eta_1{}^5 \xi_2 - 5\eta_1{}^2 \xi_{10}\right)\right), \quad \delta_3 = 36\alpha_1{}^2 \left(5\xi_7 + \alpha_1{}^2 \eta_1 \xi_{20}\right),$$

$$\delta_4 = -36\alpha_1 \left(\alpha_1{}^2 \eta_1 \xi_{21} + 5\xi_{16}\right),$$

$$\delta_5 = -3\alpha_1{}^2 \left(72\eta_1 \xi_3{}^2 + 2\eta_1{}^6 \xi_{25} - 20\eta_1{}^3 \xi_{22} + 5\xi_{12} \xi_{13}\right),$$

$$\delta_6 = 36\delta_1{}^2, \quad \delta_7 = -12\alpha_1 \delta_1 \left(-5\xi_6 + 18\eta_1 \xi_3 + 2\eta_1{}^6 \xi_2 - 10\eta_1{}^3 \xi_{10}\right),$$

$$\delta_8 = \alpha_1{}^2 \left(-5\xi_6 + 18\eta_1 \xi_3 + 2\eta_1{}^6 \xi_2 - 10\eta_1{}^3 \xi_{10}\right)^2.$$

References

[1] D.A. Nield and A. Bejan. *Convection in Porous Media*. Springer, New York, 2006.

[2] H.P.G. Darcy. *Les Fontaines Publiques de la Ville de Dijon*. Victor Delmont, Paris, 1856.

[3] H.C. Brinkman. A calculation of viscous force exerted by flowing fluid on dense swarm of particles. *Applied Science Research*, 1:27–34, 1949. doi: 10.1007/BF02120313.

[4] D.D. Joseph and L.N. Tao. The effect of permeability on the slow motion of a porous sphere. *Journal of Applied Mathematics and Mechanics*, 44(8-9):361–364, 1964. doi: 10.1002/zamm.19640440804.

[5] D.N. Sutherland and C.T. Tan. Sedimentation of a porous sphere. *Chemical Engineering Science*, 25(12):1948–1950, 1970. doi: 10.1016/0009-2509(70)87013-0.

[6] M.P. Singh and J.L. Gupta. The effect of permeability on the drag of a porous sphere in a uniform stream. *Journal of Applied Mathematics and Mechanics*, 51(1):27–32, 1971. doi: 10.1002/zamm.19710510103.

[7] I.P. Jones. Low Reynolds number flow past a porous spherical shell. *Mathematical Proceedings of the Cambridge Philosophical Society*, 73(1):231–238, 1973. doi: 10.1017/S0305004100047642.

[8] G. Neale, N. Epstein, and W. Nader. Creeping flow relative to permeable spheres. *Chemical Engineering Science*, 28(10):1865–1874, 1973. doi: 10.1016/0009-2509(73)85070-5.

[9] V.M. Shapovalov. Viscous fluid flow around a semipermeable particle. *Journal of Applied Mechanics and Technical Physics*, 50(4):584–588, 2009. doi: 10.1007/s10808-009-0079-x.

[10] G.S. Beavers and D.D. Joseph. Boundary conditions at a naturally permeable wall. *Journal of Fluid Mechanics*, 30(1):197–207, 1967. doi: 10.1017/S0022112067001375.

[11] P.G. Saffman. On the boundary condition at the surface of a porous medium. *Studies in Applied Mathematics*, 50(2):93–101, 1971. doi: 10.1002/sapm197150293.

[12] S. Khabthani, A. Sellier, and F. Feuillebois. Lubricating motion of a sphere towards a thin porous slab with Saffman slip condition. *Journal of Fluid Mechanics*, 867:949–968, 2019. doi: 10.1017/jfm.2019.169.

[13] M.C. Lai, M.C. Shiue, and K.C. Ong. A simple projection method for the coupled Navier-Stokes and Darcy flows. *Computational Geosciences*, 23:21–33, 2019. doi: 10.1007/s10596-018- 9781-1.

[14] J. Happel and H. Brenner. *Low Reynolds Number Hydrodynamics*. Englewood Cliffs New Jork, Prentice-Hall, 1965.

[15] J. Happel. Viscous flow in multiparticle systems: slow motion of fluids relative to beds of spherical particles. *American Institute of Chemical Engineers Journal*, 4(2):197–201, 1958. doi: 10.1002/aic.690040214.

[16] S. Kuwabara. The forces experienced by randomly distributed parallel circular cylinders or spheres in a viscous flow at small Reynolds numbers. *Journal of the Physical Society of Japan*, 14(4):527–532,1959. doi: 10.1143/JPSJ.14.527.

[17] S.B. Chen and X. Ye. Boundary effect on slow motion of a composite sphere perpendicular to two parallel impermeable plates. *Chemical Engineering Science*, 55(13):2441–2453, 2000. doi: 10.1016/S0009-2509(99)00509-6.

[18] D. Srinivasacharya. Motion of a porous sphere in a spherical container. *Comptes Rendus Mécanique*, 333(8):612–616, 2005. doi: 10.1016/j.crme.2005.07.017.

[19] S.I. Vasin, A.N. Fillipov, and V.M. Starov. Hydrodynamic permeability of membranes built up by particles covered by porous shells: Cell models. *Advances in Colloid Interface Science*, 139(1-2):83–96, 2008. doi: 10.1016/j.cis.2008.01.005.

[20] P.K. Yadav, A. Tiwari, S. Deo, A. Filippov, and S. Vasin. Hydrodynamic permeability of membranes built up by spherical particles covered by porous shells: effect of stress jump condition. *Acta Mechanica*, 215:193–209, 2010. doi: 10.1007/s00707-010-0331-8.

[21] J. Prakash, G.P. Raja Sekhar, and M. Kohr. Stokes flow of an assemblage of porous particles: stress jump condition. *Zeitschrift für angewandte Mathematik und Physik*, 62:1027–1046, 2011. doi: 10.1007/s00033-011-0123-6.

[22] E.I. Saad. Stokes flow past an assemblage of axisymmetric porous spherical shell-in-cell models: effect of stress jump condition. *Meccanica*, 48:1747–1759, 2013. doi: 10.1007/s11012-013-9706-y.

[23] J. Prakash and G.P. Raja Sekhar. Estimation of the dynamic permeability of an assembly of permeable spherical porous particle using cell model. *Journal of Engineering Mathematics*, 80:63–73, 2013. doi: 10.1007/s10665-012-9580-y.

[24] M.K. Prasad and T. Bucha. Creeping flow of fluid sphere contained in a spherical envelope: magnetic effect. *SN Applied Science*, 1(12):1594, 2019. doi: 10.1007/s42452-019-1622-x.

[25] M.K. Prasad and T. Bucha. Magnetohydrodynamic creeping flow around a weakly permeable spherical particle in cell models. *Pramana – Journal of Physics*, 94(1):1–10, 2020. doi: 10.1007/s12043-019-1892-2.

[26] M.K. Prasad and T. Bucha. MHD viscous flow past a weakly permeable cylinder using Happel and Kuwabara cell models. *Iranian Journal of Science and Technology Transaction A: Science*, 44:1063–1073, 2020. doi: 10.1007/s40995-020-00894-4.

[27] D. Khanukaeva. Filtration of micropolar liquid through a membrane composed of spherical cells with porous layer. *Theoretical and Computational Fluid Dynamics*, 34(3):215–229, 2020. doi: 10.1007/s00162-020-00527-x.

[28] M.K. Prasad. Boundary effects of a nonconcentric semipermeable sphere using Happel and Kuwabara cell models. *Applied and Computational Mechanics*, 15:1–12, 2021. doi: 10.24132/acm.2021.620.

[29] G.G. Stokes. On the effect of the internal friction of fluids on the motion of pendulums. *Proceedings of Cambridge Philosophical Society*, 9:8–106, 1851.

[30] C.R. Reddy and N. Kishore. Momentum and heat transfer phenomena of confined spheroid particles in power-law liquids, *Industrial and Engineering Chemical Research*, 53(2):989–998, 2014. doi: 10.1021/ie4032428.

[31] A. Acrivos and T.D. Taylor. The Stokes flow past an arbitrary particle: the slightly deformed sphere. *Chemical Engineering Science*, 19(7):445–451, 1964. doi: 10.1016/0009-2509(64)85071-5.

[32] H. Ramkissoon. Stokes flow past a slightly deformed fluid sphere, *Journal of Applied Mathematics and Physics*, 37:859–866, 1986. doi: 10.1007/BF00953677.

[33] D. Palaniappan. Creeping flow about a slightly deformed sphere. *Zeitschrift für angewandte Mathematik und Physik*, 45:832–838, 1994. doi: 10.1007/BF00942756.

[34] G. Dassios, M. Hadjinicolaou, F.A. Coutelieris, and A.C. Payatakes. Stokes flow in spheroidal particle-in-cell models with Happel and Kuwabara boundary conditions. *International Journal of Engineering Science*, 33(10):1465–1490, 1995. doi: 10.1016/0020-7225(95)00010-U.

[35] H. Ramkissoon. Slip flow past an approximate spheroid. *Acta Mechanica*, 123:227–233, 1997. doi: 10.1007/BF01178412.

[36] T. Zlatanovski. Axi-symmetric creeping flow past a porous prolate spheroidal particle using the Brinkman model. *The Quarterly Journal of Mechanics and Applied Mathematics*, 52(1):111–126, 1999. doi: 10.1093/qjmam/52.1.111.

[37] S. Deo and S. Datta. Slip flow past a prolate spheroid. *Indian Journal of Pure and Applied Mathematics*, 33(6):903–909, 2002.

[38] P. Vainshtein, M. Shapiro, and C. Gutfinger. Creeping flow past and within a permeable spheroid. *International Journal of Multiphase Flow*, 28(12):1945–1963, 2002. doi: 10.1016/S0301-9322(02)00106-4.

[39] H. Ramkissoon and K. Rahaman. Wall effects on a spherical particle. *International Journal of Engineering Science*, 41(3-5), 283–290, 2003. doi: 10.1016/S0020-7225(02)00209-4.

[40] S. Senchenko and H.J. Keh. Slipping Stokes flow around a slightly deformed sphere. *Physics of Fluids*, 18(8):088104, 2006. doi: 10.1063/1.2337666.

[41] D. Srinivasacharya. Flow past a porous approximate spherical shell, *Zeitschrift für angewandte Mathematik und Physik*, 58, 646–658, 2007. doi: 10.1007/s00033-006-6003-9.

[42] Y.C. Chang and H.J. Keh. Translation and rotation of slightly deformed colloidal spheres experiencing slip. *Journal of Colloid and Interface Science*, 330:201–210, 2009. doi: 10.1016/j.jcis.2008.10.055.

[43] E.I. Saad. Translation and rotation of a porous spheroid in a spheroidal container. *Canadian Journal of Physics*, 88(9):689–700, 2010. doi: 10.1139/P10-040.

[44] E.I. Saad. Stokes flow past an assemblage of axisymmetric porous spheroidal particle in cell models. *Journal of Porous Media*, 15(9):849–866, 2012. doi: 10.1615/JPorMedia.v15.i9.40.

[45] D. Srinivasacharya and M.K. Prasad. Axisymmetric creeping motion of a porous approximate sphere with an impermeable core. *The European Physics Journal Plus*, 128(1):9, 2013. doi: 10.1140/epjp/i2013-13009-1.

[46] D. Srinivasacharya and M.K. Prasad. Creeping motion of a porous approximate sphere with an impermeable core in a spherical container. *European Journal of Mechanics – B/Fluids*, 36:104–114, 2012. doi: 10.1016/j.euromechflu.2012.04.001.

[47] D. Srinivasacharya and M.K. Prasad. Axisymmetric motion of a porous approximate sphere in an approximate spherical container. *Archive of Mechanics*, 65(6):485–509, 2013.

[48] K.P. Chen. Fluid extraction from porous media by a slender permeable prolate-spheroid. *Extreme Mechanics Letter*, 4:124–130, 2015. doi: 10.1016/j.eml.2015.06.001.

[49] M. Rasoulzadeh and F.J. Kuchuk. Effective permeability of a porous medium with spherical and spheroidal vug and fracture inclusions. *Transport in Porous Media*, 116:613–644, 2017. doi: 10.1007/s11242-016-0792-x.

[50] P.K. Yadav, A. Tiwari, and P. Singh. Hydrodynamic permeability of a membrane built up by spheroidal particles covered by porous layer. *Acta Mechanica*, 229:1869–1892, 2018. doi: 10.1007/s00707-017-2054-6.

[51] M.K. Prasad and T. Bucha. Steady viscous flow around a permeable spheroidal particle. *International Journal of Applied and Computational Mathematics*, 5:109, 2019. doi: 10.1007/s40819-019-0692-1.

[52] M.K. Prasad and T. Bucha. Effect of magnetic field on the slow motion of a porous spheroid: Brinkman's model. *Archive of Applied Mechanics*, 91:1739–1755, 2021. doi: 10.1007/s00419-020-01852-7.

[53] J.D. Sherwood. Cell models for suspension viscosity. *Chemical Engineering Science*, 61(10):6727–6731, 2006. doi: 10.1016/j.ces.2006.07.016.

[54] A. Tiwari, P.K. Yadav, and P. Singh. Stokes flow through assemblage of non homogeneous porous cylindrical particle using cell model technique. *National Academy of Science Letters*, 41(1):53–57, 2018. doi: 10.1007/s40009-017-0605-y.

[55] H.H. Sherief, M.S. Faltas, and E.I. Saad. Slip at the surface of an oscillating spheroidal particle in a micropolar fluid. *ANZIAM Journal*, 55(E):E1–E50, 2013. doi: 10.21914/anziamj.v55i0.6813.